CyclePro: A Robust Framework for Domain-Agnostic Gait Cycle Detection

Yuchao Ma, *Student Member, IEEE*, Zhila Esna Ashari, *Student Member, IEEE*, Mahdi Pedram, *Student Member, IEEE*, Navid Amini, *Member, IEEE*, Daniel Tarquinio, Kouros Nouri-Mahdavi, Mohammad Pourhomayoun, *Member, IEEE*, Robert D. Catena, and Hassan Ghasemzadeh, *Senior Member, IEEE*

***Abstract*— The utility of wearable sensors for continuous gait monitoring has grown substantially, enabling novel applications on mobility assessment in healthcare. Existing approaches for gait cycle detection rely on predefined or experimentally tuned platform parameters and are often platform specific, parameter sensitive, and unreliable in noisy environments with constrained generalizability. To address these challenges, we introduce CyclePro,[1] a novel framework for reliable and platform-independent gait cycle detection. CyclePro offers unique features: 1) it leverages physical properties of human gait to learn model parameters; 2) captured signals are transformed into signal magnitude and processed through a normalized cross-correlation module to compensate for noise and search for repetitive patterns without predefined parameters; and 3) an optimal peak detection algorithm is developed to accurately find strides within the motion sensor data. To demonstrate the efficiency of CyclePro, three experiments are conducted: a clinical study including a visually impaired group of patients with glaucoma and a control group of healthy participants; a clinical study involving children with Rett syndrome; and an experiment involving healthy participants. The performance of CyclePro is assessed under varying platform settings and demonstrates to maintain over 93% accuracy under noisy signal, varying bit resolutions, and changes in sampling frequency. This translates into a recall of 95.3% and a precision of 93.4%, on average. Moreover, CyclePro can detect strides and estimate cadence using data from different sensors, with accuracy higher than 95%, and it is robust to random sensor orientations with a recall of 91.5% and a precision of 99.2%, on average.**

Manuscript received October 22, 2018; revised December 27, 2018; accepted January 2, 2019. Date of publication January 17, 2019; date of current version April 17, 2019. This work was supported in part by the National Science Foundation under Grant CNS-1566359 and Grant CNS-1750679, and in part by the Grant from Rett Syndrome Research Trust. The associate editor coordinating the review of this paper and approving it for publication was Prof. Chang-Hee Won. *(Corresponding author: Zhila Esna Ashari.)*

Y. Ma, Z. Esna Ashari, M. Pedram, and H. Ghasemzadeh are with the School of Electrical Engineering and Computer Science, Washington State University, Pullman, WA 99164 USA (e-mail: yuchao.ma@wsu.edu; z.esnaashariesfahan@wsu.edu; mahdi.pedram@wsu.edu; hassan.ghasemzadeh@wsu.edu).

N. Amini and M. Pourhomayoun are with the Computer Science Department, California State University, Los Angeles, CA 90095 USA (e-mail: namini@calstatela.edu; mpourho@calstatela.edu).

D. Tarquinio is with the Psychiatry and Neurology Center for Rare Neurological Diseases, Norcross, GA 30093 USA (e-mail: daniel@rareneuro.com).

K. Nouri-Mahdavi is with the UCLA Stein Eye Institute, Los Angeles, CA 90032 USA (e-mail: nouri-mahdavi@jsei.ucla.edu).

R. D. Catena is with the College of Education, Washington State University, Pullman, WA 99164 USA (e-mail: robert.catena@wsu.edu).

Digital Object Identifier 10.1109/JSEN.2019.2893225

[1]Software code and sample datasets for CyclePro are publicly available at https://github.com/y-max/CyclePro

***Index Terms*— Wearable computing, gait cycle detection, reliability, glaucoma, Rett syndrome.**

I. Introduction

With the proliferation of wearable devices, these technologies have witnessed significant attention recently due to their potential for a large number of applications in healthcare and wellness [1]. By providing real-time, objective and remote monitoring, wearable sensors have been adopted in several application domains such as human gesture recognition, in-home patient monitoring, emergency medical services, and other motion analysis applications [2]–[4]. Physical activity monitoring is one of the most important interventions in managing chronic diseases, such as cancer, diabetes, heart disease and mental health problems and it is suggested that utilizing wearable sensors to track human motions can improve the quality of life in patients with these kinds of diseases [5]–[7].

Human gait recognition and analysis is one aspect of physical activity monitoring and is possible through tracking human motion. Gait analysis reflects one's mobility and motion patterns and properties. Gait analysis can be used to examine the changes of health conditions in human subjects [8], [9]. Therefore, a number of researchers have applied gait analysis approaches in the study of motion disorders caused by various diseases, such as Alzheimer [10], Parkinson [11], [12], Glaucoma [13]–[15] and other visual impairments [16]. Thus, applications of gait analysis using wearable sensors in such areas has increasingly expanded and many researchers have focused on gait analysis, gait phases extraction, and cycle segmentation [17], [18]. However, one of the primary and fundamental steps of gait analysis is to detect gait cycles, which is the focus of this article. Efficient detection of strides can lead to extracting other important gait parameters such as mean stride speed and cadence.

Multiple algorithms have been proposed for gait cycle detection from wearable sensor signals [10], [18]–[30]. However, there have been different limitations associated with some of the existing methods. One of the limitations is the required manual observation, used to determine the alignment of multiple axial signals according to the orientation of sensor device, which limits automatic and real-time gait analysis. It is needed to manually observe the physical alignments of 3D sensor signals that is necessary to pick one specific dimension

for further analysis (i.e., vertical axis). For example, in one study [19], only x-axis acceleration signal (corresponding to the vertical direction in this case) is used in the analysis, because it is more discriminant as compared to y- and z-axis signals. Another type of manual observation aims to seek for the most appropriate variables needed in the algorithm and manually tune a threshold or inner parameter of the algorithms for each experimental setting. For example, the gait recognition method introduced in [20] requires visual detection of the first zero point in the preprocessed vertical acceleration signal. Also, some methods depend on the orientation of the wearable sensor device [18], [30]. Furthermore, many current algorithms use empirically predefined thresholds or experimentally tuned platform parameters [10], [21]. Although such gait cycle detection methods have been proven to be well-designed and practically accurate, they require fixed and predefined thresholds or parameters of gait detection platform tuned to best fit the certain experimental setting and require retraining of the gait monitoring algorithms when a new sensor platform is utilized by the end users. Also, some methods are based on standard peak detection, in which a threshold for signal peak is needed for cycle detection [22]. In addition, some methods are designed to use data from a specific type of sensor or group of sensors [18], [23], [24], [30] or data from both legs [25]. Moreover, some past work has used cross-correlation and dynamic time warping for gait detection, which needs a reference segmented gait signal [26]–[28].

To achieve a reliable and generalizable gait cycle detection approach and to overcome the aforementioned limitations, it is necessary to develop novel techniques that can work effectively in uncontrolled environments, which is the focus of this article. In this way, the methodology would not depend on observations, thresholds, type of sensor, or platform characteristics, and can learn the model parameters and adjust them with changes of sensor platform properties; such as: bit resolution, sampling frequency, signal dynamic range and sensor orientation.

In this article, we introduce CyclePro, a generic, computationally simple, and platform-independent framework for gait cycle detection. The main contributions in this article can be summarized as: (1) we introduce a reliable stride detection and cadence estimation approach, which can be applied to signals from different sensor types and is robust to random sensor orientations with no dependency on manual observations required in prior studies; (2) the proposed framework leverages physical properties of human gait to be able to learn model parameters; (3) we develop several algorithms for template generation, template matching, and optimal peak detection to find repetitive patterns and strides within the motion sensor data; (4) we demonstrate the robustness of our approach using three datasets collected with glaucoma patients, Rett patients and healthy participants. Moreover, our approach demonstrates high ($> 90\%$) accuracy under noisy signals, changes in sensor orientation, and varying sensor type, bit resolution, signal amplitude and sampling frequency of the signal.

A preliminary version of this manuscript was presented in [14] focusing on considering human physical constraints for calculating gait parameters using template generation and cross-correlation. The current manuscript has been extensively extended and enhanced, in order to achieve the optimal gait parameters by refining the preliminary results calculated using the steps in [14]. Moreover, the robustness of the new algorithm is improved and tested in regards to various platform factors and also, new datasets were used for further validations.

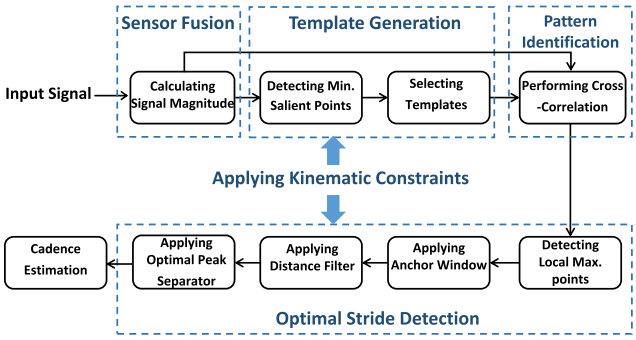

Fig. 1. High level overview of sensor data processing pipeline in the CyclePro framework.

The developed aspects of CyclePro in comparison to [14] are in multiple fronts: The previous work was based on template generation and cross-correlation, while in this manuscript, in addition to steps based on template generation and cross-correlation, a new framework of three-step optimal stride detection that was inspired by Otsu's algorithm was introduced, and it is proved to achieve a higher precision overall than the previously designed algorithm; more clinical data is collected with additional participants with glaucoma for validation of the algorithm's performance; a new clinical experiment is conducted using a customized foot-worn sensing systems to collect gait data from Rett Syndrome patients to show the robustness of algorithm to source of data; a new experiment is conducted to collect data simultaneously from six Shimmer nodes attached on lower limbs with different orientations during a normal walk test, for the purpose of evaluating the performance of our algorithm on the random orientated device without manual observations; in addition to the platform parameters tested in the previous study, we modified the original clinical dataset of Glaucoma study to simulate several signal sets with low bit resolutions in order to test the potential of our algorithm to be utilize in the wireless sensor system with power constraints.

II. CyclePro Framework Overview

As described above, stride detection is central to monitoring human gait. As soon as gait strides are accurately detected, gait parameters such as the number of strides, walking speed, and cadence can be acquired subsequently. In this article, we focus specifically on stride detection and cadence estimation. Figure 1 presents a high level overview of the processing pipeline for CyclePro framework.

TABLE I
PHYSICAL CONSTRAINTS OF NORMAL CADENCE

Notation	Definition	Value
C_{mean}	Average number of strides per minute for a normal walk	50
C_{max}	Upper bound on the range of the normal cadence	65
C_{min}	Lower bound on the range of the normal cadence	40
C_{over}	Extreme high cadence that is more likely for running rather than normal walk	70

A. CyclePro Architecture

The input signals of CyclePro are collected from wearable sensors mounted on both feet or embedded in shoes. These body sites are suggested to be effective for gait monitoring [31]–[33]. The wearable sensors include motion sensors such as accelerometer and gyroscope, as well as electronic sensors like force sensitive resistor (i.e. pressure sensor). The proposed algorithms in CyclePro contains four major phases:

- Sensor Fusion: Calculating the Signal Vector Magnitude to reduce the complexity in the raw signals.
- Template Generation: Generating templates of one gait cycle (stride) using the Signal Vector Magnitude, by automatically computing the required window-size for representing a template.
- Pattern Identification: Capturing repetitive patterns in the signal using a normalized cross-correlation approach by taking into account the kinematic properties of human gait.
- Optimal Stride Detection: Detecting the strides accurately using algorithms which automatically compute required window sizes as well.

In the rest of this section, we first introduce several kinematic constraints of human gait, and then discuss the contribution of individual signal processing modules to the robustness of the proposed framework. In the end, we describe each of the aforementioned modules in detail, and also explain the cadence estimation approach used in this study.

B. Kinematic Constraints

Given the fact that biometric gait behavior is one type of physical motion, it is constrained to several physical conditions. Such restrictions can be used in gait monitoring given the correlation between kinematic measurements and spatio-temporal signals generated during ambulation. Table I outlines several kinematic constraints for normal cadence measured by prior clinical research [34]–[36].

We utilize these statistics of normal walk cadence (strides/minute) to automatically adjust the internal parameters of our algorithm. As it will be discussed later in this paper, these parameters define the lower bound on the size of anchor window and distance filter.

C. Robustness Features

In order to explain the robustness property of CyclePro, we highlight four methods used in our algorithm design as shown in Table II. Applying these methods in CyclePro results in six properties of the proposed framework, which are denoted as the labels shown in the third column of Table II. The explanation for each property is listed in Table III.

TABLE II
METHODS APPLIED IN CYCLEPRO ALGORITHM DESIGN

No.	Methods	Effects (Labels)
1	Considering physical constraints	A, D
2	Using Signal Vector Magnitude	B, F
3	Applying normalized cross-correlation	A, C, E, F
4	Performing optimal peak detection	A

TABLE III
MAJOR PROPERTIES OF CYCLEPRO FRAMEWORK ATTRIBUTED TO METHODS IN TABLE II

Label	Properties
A	Free of predefined thresholds
B	Robust to random sensor orientation
C	Robust to the changes of bit resolution
D	Robust to the changes of sampling frequency
E	Robust to signal amplitude
F	Reliable for the noisy signal readings

III. CYCLEPRO FRAMEWORK DESIGN

This section provides detailed explanation of major phases in the CyclePro framework, as it is mentioned in the previous section. For visualization purpose, Figure 2 shows the step-wise results of signal processing in CyclePro using a sample accelerometer signal.

A. Sensor Fusion

As mentioned previously, the first step of the algorithm is to calculate Signal Vector Magnitude according to the sensor signals collected from three-dimentional accelerometer or three-dimentional gyroscope. The computation of Signal Vector Magnitude is defined by equation (1). For signals collected from pressure sensor, the same equation can be applied with $x = y = z$.

$$SignalVectorMagnitude = \sqrt{x^2 + y^2 + z^2} \qquad (1)$$

As mentioned previously, there are several advantages of using the Signal Vector Magnitude instead of the original sensor signals. For instance, the Signal Vector Magnitude reflects the overall intensity of user's movement as a sequence of positive values, and hence, it highlights the cyclic patterns while neutralizing the noise in uni-axial signals. In addition, it is not necessary to distinguish each individual axial signal even if the sensor orientation changes. As a result, the algorithm does not need manual annotation for the physical alignments of three axial signals, and the reduction of the input dimensionality also helps the system scalability and real-time processing applications. Figure 2 shows the Signal

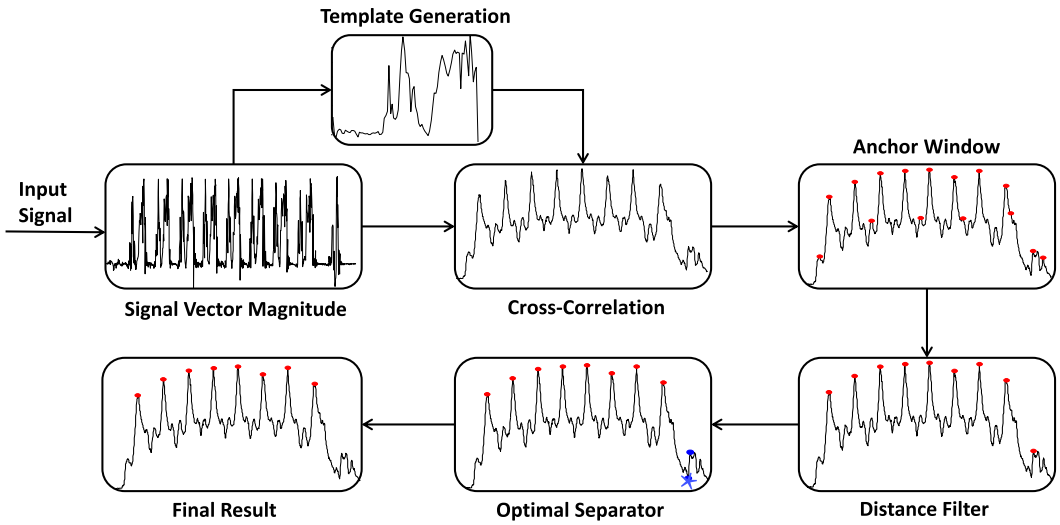

Fig. 2. Evolution of the sample input accelerometer signal in each step of CyclePro framework, showing the final detected strides in Final Results (red circles showing detected peaks and blue asterisk representing the inserted minimum valley point).

Vector Magnitude of a randomly selected experimental signals recorded using an accelerometer sensor.

B. Template Generation

In this step, the templates of repetitive pattern with respect to one gait cycle are generated in Signal Vector Magnitude signal. A template is a signal segment determined by two consecutive minimum salient points, and each template accounts for approximately one gait cycle. Salient points are data samples with local minimum amplitude, and the procedure of selecting these points is described in [14]. For this purpose, we use salience point vector. In this vector, there is one value for each data sample in the signal sequence, which denotes the number of following consecutive data samples with larger amplitude than that of the current data sample. Salience point vector is used to detect salient points, which are data samples with local minimum amplitude and have been separated by gait events covering one step.

After generating templates using obtained salient points, we compare the standard deviation of each template with the entire signal sequence, and select the top three templates which have the smallest difference in standard deviation. Figure 2 shows one of the three automatically selected templates from the given Signal Vector Magnitude signal.

C. Pattern Identification

In this step, the cross-correlation function is adopted, which takes each selected template as the input, and continuously estimates the similarity between each template and the entire Signal Vector Magnitude signal sequence. CyclePro employs normalized cross-correlation to bound the maximum value to 1. Therefore, the output is not sensitive to the changes of amplitude range in original signal. Moreover, this approach enhances the overall reliability of algorithm, as mentioned in Table II and III. Equation (2) describes normalized cross-correlation function used in this phase, where N and T denotes the number of data samples in the signal sequence and the template respectively, while $A_s(j)$ and $A_t(j)$ denotes the amplitude of the jth data sample in the signal and in the template, respectively.

$$C(i) = \frac{\sum_{j=1}^{T} A_t(j) A_s(j+i)}{\sum_{j=1}^{T} (A_t(j))^2}, \quad i \in [0, N-T] \tag{2}$$

The output obtained from this step is shown in the box named “Cross-Correlation” in Fig. 2 using a sample signal.

D. Optimal Stride Detection

The output sequence of normalized cross-correlation is then used as the input for optimal stride detection module. First off, this module recursively finds local maximum data points that have higher amplitude than the neighboring points in the sequence. The selected data points are then passed through three steps for the final stride detection. For clarification, the terms and notations listed in Table IV are used throughout the rest of this section.

The three steps in this module includes *anchor window*, *distance filter*, and *optimal separator*. We elaborate each of these steps as follows.

1) Anchor Window: In the first step, an anchor window is defined as a dynamic window that iteratively moves in the list of extracted local maximum data points, from the first data point to the last one. In each iteration, the anchor window algorithm projects a window with certain size from the starting data point, and seeks for the data point in the sequence with the highest cross-correlation result within this window. It then removes other local maximum points obtained previously which lies inside the current window, and projects another anchor window from the next local maximum data point. Algorithm 1 presents the pseudocode for this step.

The size of the anchor window is determined by the parameter N_{step} according to the average value of normal walk cadence listed in Table I. Considering the fact that one

TABLE IV
NOTATIONS USED IN STRIDE DETECTION ALGORITHMS

Terms	Definition
L_i	The i^{th} sample point in a list L
$L_{i,j}$	A sequence of sample points from the i^{th} to the j^{th} in list L
$\|L_i,L_j\|$	The distance of L_i and L_j, measured by the number of sample points between them in the signal
A_s	The start point of current anchor window
A_p	The point with largest amplitude within current anchor window
N_{step}	Number of signal samples used to depict one step in the normal cadence, estimated by $(60 \times f/C_{mean} \times 2)$
f	Sampling frequency of acceleration signal
a(x)	The amplitude of sample point x
μ	The mean value of a given list
$\sigma_{i,j}{}^2$	The variance of the value from the i^{th} to the j^{th} sample points in a given list

Algorithm 1 Anchor Window Algorithm

Input: list L of local maximum samples in the cross-correlation output
$A_s \leftarrow L_1$
for j is $2 \rightarrow |L|$ **do**
  $A_p \leftarrow A_s$
  while $| A_s, L_j | < N_{step}$ **do**
    $A_p \leftarrow$ the sample point with larger amplitude between current A_p and L_j
    $j \leftarrow j + 1$
  end while
  Add A_p into P_{out}
  $A_s \leftarrow L_j$
end for
Output: P_{out} the list containing the peak sample point of each anchor window

stride usually contains two steps, the number of data samples required to capture one stride needs to be twice of the number used for one step. Therefore, we use the latter number to restrict the interval of each possible stride under search. The box named "Anchor Window" in Fig. 2 shows the result of this step, where the points marked with red circle indicate the selected local maximum points.

2) Distance Filter: This step is developed to further examine those local maximum points obtained from the previous step. We use equation (3) for the filtering purpose, which indicates the number of data samples used to capture one stride in the movement that is more likely to be running than normal walk.

$$N_{stride} = \frac{60 \times f}{C_{over}} \tag{3}$$

Since N_{stride} is used to represent running, it can refer to a lower bound of the temporal distance between every two consecutive strides of a normal walk. Distance filter works in this way that, for each pair of consecutive local maximum points in P_{out}, if the number of data points in the sequence between them is less than N_{stride}, only the one with higher value in this pair is selected for the later procedure, whereas another one is filtered out. The result of this step is shown in the box named "Distance Filter" in Fig. 2.

Algorithm 2 Optimal Peak Separator Algorithm

Input: list P of peak sample points returned by distance filter, minimum valley point v
$P \leftarrow$ sort P according to sample values in descending order
Add v into P
$n \leftarrow$ the number of sample points in P
$var \leftarrow \sigma^2_{1,n} = \sum_{i=1}^{n} \frac{(a(P_i)-\mu)^2}{n-1}$
$k \leftarrow 1, b \leftarrow n$
for k is $1 \rightarrow n$ **do**
  if $\sigma^2_{1,k} + \sigma^2_{k+1,n} < var$ **then**
    $var \leftarrow \sigma^2_{1,k} + \sigma^2_{k+1,n}$
    $b \leftarrow k$
  end if
end for
$P_{final} \leftarrow P_{1,b}$
Output: P_{final} the list of selected final peaks

3) Optimal Peak Separator: This step aims to automatically determine the final peaks (local maximum) based on the similarity determined by the cross-correlation results. To avoid any fixed threshold, we design an optimal separator algorithm inspired by Otsu's method, which is commonly used in image processing for the purpose of image segmentation [37]. This method exhaustively derives an optimal threshold to minimize the sum of inner variance over all the image segments and thus, to separate them. It can also be used over the results of filtered local maximum points, to separate valid and invalid peaks for final output.

However, since human movement pattern changes inconspicuously within a short time interval, there can be slight fluctuations in the amplitude of adjacent data samples, which would affect the results of cross-correlation. Therefore, by only considering the inner variance to separate the points, we may reject a valid peak associated with a real stride due to its slightly lower cross-correlation result than the others. In order to address this issue and reduce the false negative rate, we insert a point named "minimum valley" into the filtered local maximum points as the baseline, to balance the comparison of the inner variance. Minimum valley is the data point with the smallest value among all the valleys in the sequence, and it is denoted as variable v. The pseudocode for optimal peak separator is presented in Algorithm 2.

To use this algorithm, the resulting local maximum points from distance filter is first sorted according to the cross-correlation results, and then, an exhaustive search for an optimal separation is applied with the goal of minimizing the sum of inner variance within the two separated data point partitions.

As shown in the box named "Optimal Separator" in Fig. 2, the input for optimal peak separator step includes the points marked with circles (red and blue), which represent the peaks remained after distance filter step. The point marked with

asterisk represents the inserted minimum valley point. When the sum of inner variances within the two partitions reaches its minimum value, the blue circle-marked point and the minimum valley point are separated from the rest of data samples as a new group; therefore, the output is a collection of data samples marked with red circles. The final output of stride detection is shown in the box named "Final Result" in Fig. 2, and each peak is associated with one stride recorded in the Signal Vector Magnitude signal.

E. Cadence Estimation

After stride detection phase, we further estimate cadence based on the intervals representing the gait cycles. The cadence estimation phase follows the equation (4), where N_{intvl} denotes the number of data samples within two consecutive valid peaks.

$$Cadence = \frac{60 \times f}{N_{\text{intvl}}} \tag{4}$$

This equation calculates the cadence for every two consecutive valid peaks, and then the average value is computed as the cadence for the input signal. Furthermore, as mentioned at the beginning of this section, three different templates are generated and used by the algorithm, which results in three sets of results in the end. Therefore, the final set of results presented by CyclePro is the average of the results achieved by each template.

IV. Experiments

For validation purpose, we conducted two clinical experiments in collaboration with medical institutes [15] and one in-lab experiment for data collection. The experiments were approved by the Institutional Review Board (IRB) of each participating institution under these reference numbers: glaucoma trials under IRB#13-000804 and Rett syndrome trials under IRB#201801242. Each experiment was done in multiple trials and the final results were presented as the average over different trials. In addition, to measure the performance of CyclePro with changes in the sensor platform, we modified one dataset to simulate a variety of sensor parameter settings.

In order to evaluate the performance of CyclePro in each experiment, we used recall and precision based on the number of strides recorded in the sensor signal that were recognized correctly, and they are defined in equations (5), (6).

$$Precision = \frac{TP}{TP + FN} \tag{5}$$

$$Recall = \frac{TP}{TP + FP} \tag{6}$$

where TP is the number of real strides recognized correctly, FN is the number of real strides that were not recognized, and FP is the number of strides that were not real but recognized incorrectly by CyclePro. Therefore, the corresponding error is related to presence/absence of any real strides in the detected strides.

The rest of this section introduces the experiments and dataset acquisition.

Fig. 3. Clinical setting used for data recording in glaucoma trial, consisting two shimmer sensors mounted on each shoe.

A. Glaucoma Trials

The first dataset was collected in a clinical study from 8 healthy participants and 8 patients with glaucoma eye-condition. Glaucoma is the second leading cause of blindness in adults, and it appears in different types [38]–[40]. Since glaucoma affects patient's vision in various levels, patient's quality of life can be harmed significantly. For example, it is known that glaucoma patients walk slower and have an increased risk of falling compared to typical sighted individuals [41]. Therefore, their gait behavior could be affected and this is the reason for considering this dataset in this manuscript.

We conducted a randomized clinical experiment involving 8 glaucoma patients (age 63.7±8.57, height 168.73±7.13 cm) and 8 age-matched healthy control (age 60.7±4.99, height 161.96±8.43 cm) [15]. All participants were asked to perform a 10-Meter-Walk test, which is a simple, effective and widely used tool to evaluate gait patterns [42], while two Shimmer (Sensing Health with Intelligence, Modularity, Mobility and Experimental Reusability) [43] sensor nodes were mounted on the top of their shoes. Signals were continuously gathered from tri-axial accelerometer (MMA7260Q) integrated in each Shimmer device. We used a sampling frequency of 102.4Hz, and the sensitivity range was set to ±2g. Figure 3 shows the experimental setup for this test as well as a shimmer sensor.

The recorded datasets were manually annotated by synchronizing with video recordings to create ground truth data for validation of experiments' results. We used the original signals to measure baseline accuracy of our gait monitoring framework. Furthermore, to test the robustness of CyclePro on the changes of sensor platform variables as well as noisy signals, we modified the original signals to acquire several datasets. We changed sampling the dataset by up-sampling and down-sampling of original signals. Furthermore, we changed its amplitude and bit resolution and added different levels of noise to the original signal. The list of various tested parameters is presented in Table V, where the asterisk denotes the parameter value in the original dataset.

It should be noted that bit resolution refers to the bit number of Analog to Digital Converter (ADC) in the microcontroller of a sensor for representing output. Sensor nodes normally have a severely limited energy budget [44]. Therefore, we modified original acceleration signals by truncating the binary raw

TABLE V

NEW DATASETS SIMULATION FOR ROBUSTNESS VALIDATION (ORIGINAL VALUES ARE MARKED WITH ASTERISKS)

Parameter	Parameter values for different datasets
Bit Resolution	16-bit*, 12-bit, 10-bit, 8-bit
Sampling Frequency	204.8Hz, 102.4Hz*, 51.2Hz, 34.1Hz, 17Hz
Signal Amplitude	0.5X, 1X*, 2X, 3X
Signal-to-Noise Ratio	20dB, 15dB, 10dB, 5dB

Fig. 4. Clinical setting of the shoe-integrated platform used for data recording in Rett trial, consisting accelerometer, gyroscope and pressure sensors in each shoe.

signals in order to simulate the digital readout with lower bit resolutions.

B. Rett Syndrome Trials

The second dataset of human gait is collected in another clinical study for patients with Rett Syndrome, in order to test the algorithm on a patient with a different health situation, and when data is recorded in a new experimental setting using a different sensor platfrom. Rett Syndrome is a rare neurological disorder that affects almost every aspect of one's daily life, such as breathing, eating, learning and walking with a wide range of disabilities from mild to severe [45]–[48]. Patients suffering from Rett Syndrome are known to have difficulties in walking.

This dataset was recorded in an experimental setting using an integrated sensors device and the gait data are gathered using three different sensor types: accelerometer, gyroscope and pressure sensors. The device was mounted on a pair of shoes and was tested by a 14 years old female patient, who had mild symptoms and thus, she was able to walk independently. We developed the hardware, software, and algorithms for collecting and analyzing gait data using a shoe-integrated platform, as shown in Fig. 4.

As shown in Fig. 4, five pressure sensors are implemented in the designed platform to gather related data of patients for different analysis and the data from sensor number one were used in this article. The inertial sensors platform allows for real-time collection of kinematic data during clinical experiments. Signals generated from sensing units are first sampled by the micro-controller while the sampling frequency was set to 26Hz for this experiment. Then, the collected data samples are transmitted to a computer from each of the shoes separately. In addition, a Windows-based user interface was

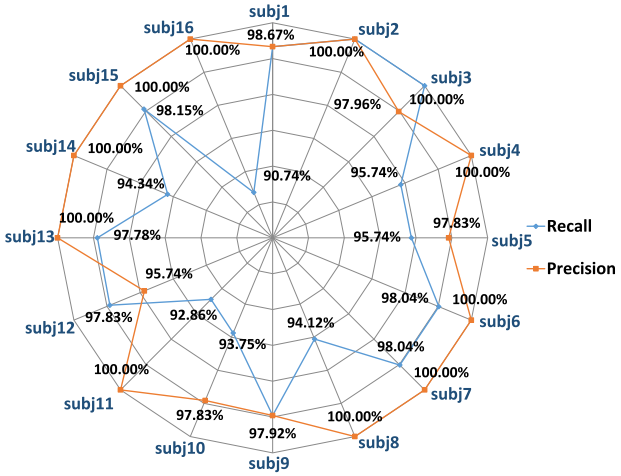

Fig. 5. Recall and precision values for stride detection using CyclePro, when applied over glaucoma dataset, (subj1 to subj13 stand for each of individual participants).

developed for real-time data collection and visualization. For clinical usage, our user interface also provides video recording function in order to simultaneously capture participant's movement during the experiment. The video recordings were automatically synchronized with the wearable sensor signal readings, which was used to annotate the data for validation of results. In this way, we could obtain ground truth data such as the time when a gait cycle is initiated, when the person is walking and when the experiment ended.

In this dataset, the 10-Meter-Walk test was used to record signals from sensors. Again, for further analysis we change the sampling frequency and noise level for accelerometer data of this dataset. In addition to original frequency of 26Hz, we tested 13Hz and 52Hz frequencies. Also, we added noise with SNR levels described in Table V to the original signal to test CyclePro's performance.

C. Sensor Orientation Test

The third dataset includes gait data recorded by an accelerometer from 4 normal participants and it is generated during a normal walk test. This dataset is used to evaluate the performance of CyclePro on random sensor orientations, since motion sensor readings vary on different directions.

To evaluate the impact of sensor orientations in addition to previous parameter settings, we conducted an independent normal walk experiment with healthy participants. For this test, each participant was asked to walk in a well-lit hallway for 20 meters at their normal speed, while three Shimmer sensors were attached on each of the lower shanks with different orientations. Four healthy participants (age 25.3±2.38, height 176.5±2.87 cm) were involved in this test and the accelerometer used in this test had the same platform settings as the one used in the first test. Acceleration signals were collected simultaneously from six Shimmer sensor nodes attached on bilateral lower shanks, while, three Shimmer devices were attached on each limb, and they were aligned with vertical, horizontal and oblique directions respectively. The datasets

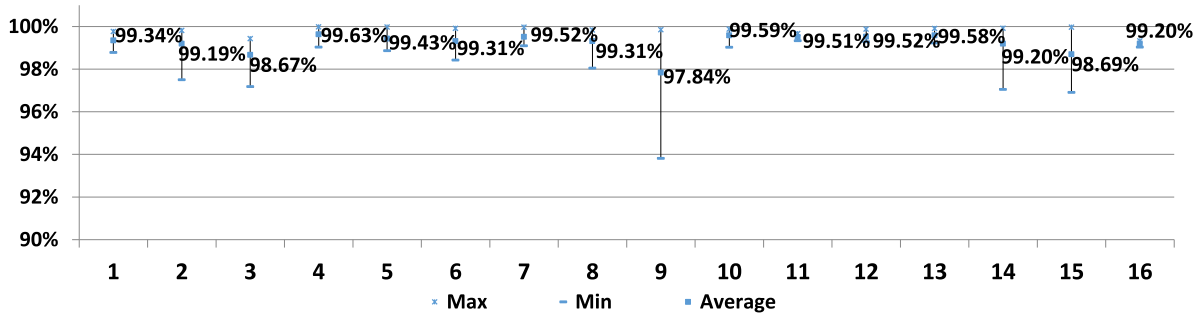

Fig. 6. Baseline results of cadence estimation using glaucoma dataset.

were manually annotated to create ground truth data for validation of results.

V. Results

A. Baseline Performance

For the first dataset, a total number of 811 strides were recorded from two accelerometers for 16 participants during the 10-Meter-Walk test. We first used the original dataset of glaucoma trial to evaluate the basic performance of CyclePro for stride detection. For evaluation purpose, the recall and precision, defined in equations (5)-(6), are calculated based on the number of strides recorded in the sensor signal that were recognized correctly, while the true real strides were determined by manual annotations done over the dataset from sensors.

The recall and precision over the entire dataset were 96.55% and 99.11% respectively, and our algorithm can achieve a recall above 90% and a precision above 95% for individual participants, as it is shown in Fig. 5 as a radar chart.

In this figure, subj1 to subj13 stand for each of individual participants and the value for recall and precision for each participants is demonstrated using circles with various radiuses.

We then evaluated the baseline performance of cadence estimation for each participant individually by comparing the results against manual annotations, as it is shown in Fig. 6. The accuracy is defined as the precision of the estimated result with respect to the annotated value. Figure 6 shows the average accuracy as well as the variations for each participant over different trials. The results demonstrate that CyclePro achieves an average accuracy above 97% in cadence estimation for both healthy and visually-impaired participants.

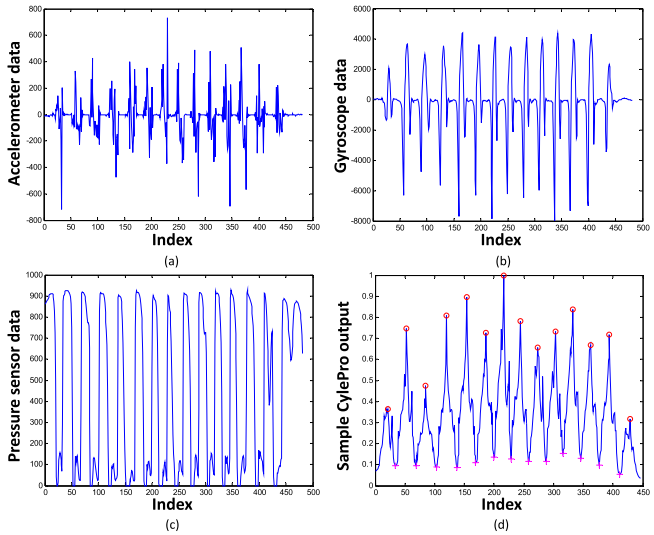

Fig. 7. An example of signal sequence collected in one Rett trial shown in sub-figures (a) to (c) and the corresponding output of CyclePro shown in sub-figure (d). Circles show detected local maximum points and crosses are for local minimum points.

TABLE VI
Results of Cadence Estimation Per Sensor Type Using Rett Dataset

Sensor	Accuracy			
	Left foot	Right foot	Max	Min
Accelerometer	97.11%	97.51%	99.72%	92.98%
Gyroscope	96.86%	97.97%	99.99%	93.75%
Pressure Sensor	96.71%	98.4%	99.92%	90.48%

B. Performance Using Different Types of Sensors

To evaluate the performance of CyclePro on the data generated by a new platform consisting of different types of sensors, we used the second dataset collected from patients with Rett Syndrome. This dataset was gathered during a 10-Meter-Walk test including three trials. Figure 7 shows an example of signal sequence generated by accelerometer, gyroscope and pressure sensor in one trial, as well as a sample output of CyclePro using one template of the signal sequence.

It can be observed that all the three signal sequences have a periodic nature, which corresponds to the repetitive gait cycles. Similar to our previous experiment, we first measured the baseline performance of CyclePro for stride detection by estimating the precision and recall on the data gathered by different sensors separately. The results are presented in Fig. 8 for both feet.

The results indicate that for all three sensors data, CyclePro keeps its high performance with the recall over 95% and the precision over 90%. Next, the baseline performance of CyclePro for cadence estimation according to different sensors was also evaluated, and the results are presented in Table VI.

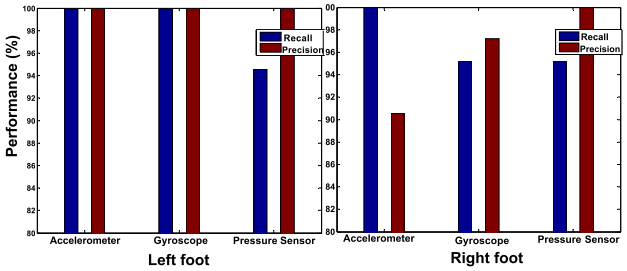

Fig. 8. Results of stride detection per sensor type using Rett dataset, for left and right feet shown in left and right plots respectively.

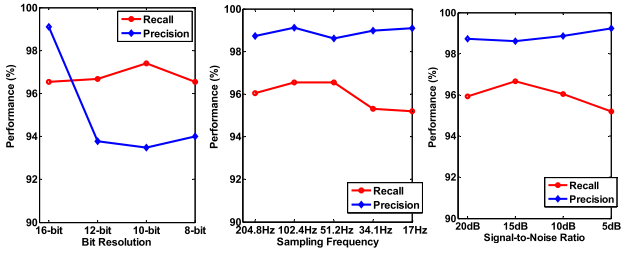

Fig. 9. Results of stride detection on datasets with parameter changes simulated using glaucoma dataset.

According to this table, the performance of CyclePro for cadence estimation remains over 90% while using different types of sensors.

C. Robustness to Platform Parameter Changes

In the following three subsections, the robustness of CyclePro to the changes in sensor parameters is assessed. We evaluated the performance for stride detection and cadence estimation on each of the simulated datasets mentioned in Table V, and Fig. 9 shows the corresponding results in terms of recall and precision.

In addition, the accuracy for cadence estimation on the simulated datasets with the minimum and maximum parameter values, are reported in Table VII and explained in the following subsections.

1) Bit Resolution Changes: A low bit resolution of wireless sensor output can reduce the power consumption, and hence, enhance the functional period of body sensor networks (BSN) [49]. Furthermore, bit resolution is a platform parameter as well as an algorithm specific parameter. Thus, we evaluate the robustness of CyclePro with changes in bit resolution of the signal. The leftmost plot in Fig. 9 shows the result of stride detection on the changes of bit resolution, which were simulated using the first dataset collected from glaucoma patients and control group. Comparing to the performance on the original dataset (16-bit), CyclePro maintains a precision above 93% and a recall above 96% and with lower bit resolutions, the drop in the accuracy is less than 6%.

By considering bit resolution changes shown in Table VII, the results demonstrate that when the number of bits used to represent raw signal are reduced to 8, CyclePro still achieves an average accuracy of 96.73% for cadence estimation. Moreover, the variance in the accuracy of cadence estimation on the four simulated datasets with different bit resolutions is 1.49.

TABLE VII

RESULTS OF CADENCE ESTIMATION ON DATASETS WITH PARAMETER CHANGES SIMULATED USING GLAUCOMA DATASET

	Bit Resolution		Sampling Rate		SNR	
	16 bit	8 bit	102.4Hz	17Hz	20dB	5dB
Accuracy(%)	99.22	96.73	99.22	98.18	99.18	99.01

2) Sampling Frequency Changes: We also tested CyclePro using several datasets obtained by upsampling/downsampling the original sensor siginals (102.4Hz) in the first dataset collected during glaucoma trials. The middle plot in Fig. 9 shows the stride detection performance on the changes; CyclePro has a performance of 95.19% recall and 99.10% precision even though the sampling frequency reduced to 17Hz. The drop in the accuracy comparing with baseline performance is less than 2% for all the datasets.

The results listed in Table VII indicate that, CyclePro maintains an average accuracy of 98.18% for cadence estimation in the condition of low sampling frequency. The variance of the performance is 0.2 over all the datasets with different sampling frequencies.

In addition, we changed the sampling frequency of accelerometer data in the second dataset collected from Rett Syndrome patient, from 26Hz to 13Hz and 52Hz, separately. The results show that, CyclePro achieves an average recall of 92.3% and precision of 100% for stride detection, and an average accuracy of 98.24 for cadence estimation, which further demonstrates the robustness of CyclePro.

3) Performance With Noisy Signal: Many gait monitoring applications nowadays are not meant to be used inside laboratory, neither do they build upon sensor platforms with precise settings. As a result, extra noise may be introduced in the sensor readouts under uncontrolled environments.

To test the reliability of CyclePro in such situations, we added different degrees of white noise into the original signals in the first dataset collected in glaucoma trials. We then performed CyclePro on each of the obtained datasets, and the rightmost plot in Fig. 9 shows the performance on these modified datasets with Signal-to-Noise Ratio (SNR) of 20dB, 15dB, 10dB and 5dB. CyclePro can maintain a recall above 95% and a precision above 98% for all these noisy signal sets. The drop in the accuracy comparing with the baseline is less than 2%.

The last two columns in Table VII show the results of cadence estimation in the noisy signals. CyclePro can achieve an accuracy above 99% and higher on noisy datasets, and the variance among all created datasets, with different SNR shown in VII, is 0.01.

We further added the same set of noises to the second dataset collected from Rett Syndrome patient. The results indicate that CyclePro could achieve an average recall of 92.57% and precision of 98.07% for stride detection, and an average accuracy of 98.62% for cadence estimation.

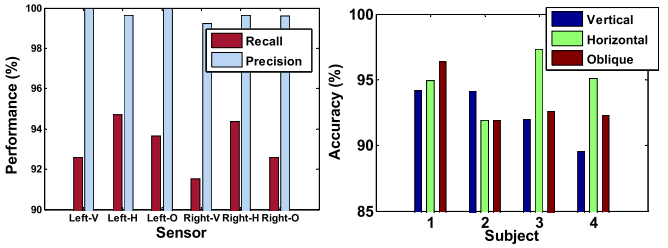

Fig. 10. Results of stride detection on datasets with different sensor orientations (L:left ankle, R: right ankle, V: vertical, H: horizontal, O: Oblique), "Performance per ankle/orientation" is shown in left plot and "Accuracy per participant" is shown in right plot.

TABLE VIII
ACCURACIES OF CADENCE ESTIMATION ON DATASETS WITH DIFFERENT SENSOR ORIENTATIONS

Subject	L-V	L-H	L-O	R-V	R-H	R-O
Sub 1	95.40%	95.76%	95.77%	95.18%	98.27%	96.55%
Sub 2	93.30%	92.62%	94.67%	92.81%	94.29%	93.94%
Sub 3	93.03%	96.33%	94.69%	93.31%	93.92%	93.31%
Sub 4	94.66%	94.90%	94.34%	90.65%	94.07%	93.79%
Average	94.10%	94.90%	94.87%	92.99%	95.14%	94.40%

D. Robustness to Signal Amplitude Changes

Due to the fact that the stride detection of CyclePro is applied on the output of normalized cross-correlation function, the result is not sensitive to the changes of signal amplitude range by default. As a result, the validation of both stride detection and cadence estimation using the datasets with different signal amplitudes turned out to be exactly same results with the baseline.

E. Robustness to Sensor Orientation Changes

As mentioned previously, the third experiment for data collection was conducted on four participants in a normal walk test, and three Shimmer sensors were attached on each of their lower shank during the experiment. Each sensor was placed in a different direction: horizontal, vertical, or oblique, and a total number of 566 strides were recorded in the acceleration signals according to manual annotation. Figure 10 shows the results of stride detection in terms of recall and precision for each sensor, and for each participant, separately.

In the left plot in Fig. 10, the x-axis refers to each sensor denoted as its location and orientation. Sensors attached on the left ankle are denoted as Left-V, Left-H and Left-O, and sensors attached on the right ankle are labeled as Right-V, Right-H and Right-O, respectively. Based on the results in Fig. 10, CyclePro delivers a precision above 99.2% and a recall above 91.5% in average for the six sensors with different locations and orientations.

The right plot in Fig. 10 shows the accuracy of stride detection according to different sensor orientations for each subject. CyclePro maintains an accuracy higher than 89.5% regardless of the differences in the sensor signals caused by the orientation changes. The overall recall and precision of orientation-insensitive stride detection is 93.23% and 99.68%, respectively.

CyclePro was also tested for cadence estimation on the datasets with different sensor orientations, and the results were compared to manual annotations. Table VIII presents the accuracy of cadence estimation using CyclePro on each individual dataset generated by one sensor for one subject. It shows that CyclePro can maintain an accuracy higher than 92% in cadence estimation for various sensor orientations. The overall accuracy of orientation-insensitive cadence estimation is 94.4%.

VI. CONCLUSION AND FUTURE WORK

In this paper, we aimed to provide an accurate and comprehensive biometric gait examination through a reliable and platform-independent data analysis approach. To this end, we introduced a robust gait cycle detection framework, named CyclePro, for stride detection and cadence estimation. Our algorithm takes human kinematic constraints into account to automatically adjust the framework parameters. These human population gait norms are used in our method to eliminate the need to tune platform parameters with any new changes. As a result, our approach detects gait cycles with no dependency on predefined platform thresholds or experiment-specific settings.

For validation purpose, we first demonstrated the performance and robustness of CyclePro on gait data collected in two clinical trials. Our goal was to assess the reliability of CyclePro on changes in bit resolution, sampling frequency, signal amplitude and noise level in signal, as well as its performance on data generated by different sensors and we used manual annotation of the data as the gold standard for our performance evaluation. We could observe that CyclePro can maintain a sufficient performance in various conditions (higher than 93% precision and 95% recall for stride detection and 96% for cadence estimation). We also conducted a normal walk experiment using randomly aligned sensor devices and collected acceleration signals simultaneously. Using the results,the reliability of CyclePro in the changes of sensor orientation (higher than 99% precision and 91% recall for stride detection and 92% for cadence estimation) could be concluded.

As some of the limitations of previous works for gait cycle detection are mentioned in Introduction section, we are able to make a comparison between those and our proposed algorithm. CyclePro does not need the alignment of multiple axial signals according to the orientation of sensor device, or seeking for the most appropriate variables such as first zero point, which is a necessary step in some proposed algorithms [19], [20]. Also, CyclePro uses human kinematic information to eliminates the need for tuning sensor platform parameters and thresholds based on experimental settings, which should be done is some previous methods [10], [21]. In addition, it is not dependent on set threshold for signal peak detection which is needed in some proposed methods [22]. Furthermore, some designed algorithms are specific to special types of sensor [23], [24] which is not the case for CyclePro. Also, some methods are dependent on data recorded by sensors worn on both legs [25], and it is not a limitation for CyclePro. Moreover, there are some methods for cycle detection that are based on

cross-correlation and dynamic time warping and they need a reference segmented gait signal [26]–[28], while CyclePro does not need a reference signal.

REFERENCES

[1] H. Ghasemzadeh and R. Jafari, "Physical movement monitoring using body sensor networks: A phonological approach to construct spatial decision trees," *IEEE Trans. Ind. Informat.*, vol. 7, no. 1, pp. 66–77, Feb. 2011.

[2] G. Yang *et al.*, "A health-IoT platform based on the integration of intelligent packaging, unobtrusive bio-sensor, and intelligent medicine box," *IEEE Trans. Ind. Informat.*, vol. 10, no. 4, pp. 2180–2191, Nov. 2014.

[3] B. Xu, L. D. Xu, H. Cai, C. Xie, J. Hu, and F. Bu, "Ubiquitous data accessing method in IoT-based information system for emergency medical services," *IEEE Trans. Ind. Informat.*, vol. 10, no. 2, pp. 1578–1586, May 2014.

[4] S. J. M. Bamberg, A. Y. Benbasat, D. M. Scarborough, D. E. Krebs, and J. A. Paradiso, "Gait analysis using a shoe-integrated wireless sensor system," *IEEE Trans. Inf. Technol. Biomed.*, vol. 12, no. 4, pp. 413–423, Jul. 2008.

[5] S. J. Lee, Y. Motai, and H. Choii, "Tracking human motion with multichannel interacting multiple model," *IEEE Trans. Ind. Informat.*, vol. 9, no. 3, pp. 1751–1763, Aug. 2013.

[6] S. J. Biddle and M. Asare, "Physical activity and mental health in children and adolescents: A review of reviews," *Brit. J. Sports Med.*, vol. 45, no. 11, pp. 886–895, 2011.

[7] S. J. Strath *et al.*, "Guide to the assessment of physical activity: Clinical and research applications: A scientific statement from the American heart association," *Circulation*, vol. 128, no. 20, pp. 2259–2279, 2013.

[8] W. Tao, T. Liu, R. Zheng, and H. Feng, "Gait analysis using wearable sensors," *Sensors*, vol. 12, no. 2, pp. 2255–2283, Dec. 2012.

[9] C.-C. Yang, Y.-L. Hsu, K.-S. Shih, and J.-M. Lu, "Real-time gait cycle parameter recognition using a wearable accelerometry system," *Sensors*, vol. 11, no. 8, pp. 7314–7326, Nov. 2011.

[10] Y.-L. Hsu *et al.*, "Gait and balance analysis for patients with Alzheimer's disease using an inertial-sensor-based wearable instrument," *IEEE J. Biomed. And Health Informat.*, vol. 18, no. 6, pp. 1822–1830, Nov. 2014.

[11] J. Barth and *et al.*, "Biometric and mobile gait analysis for early diagnosis and therapy monitoring in Parkinson's disease," in *Proc. 33rd Annu. Int. Conf. IEEE EMBS*, Boston, MA, USA, Sep. 2011, pp. 868–871.

[12] C. Caramia *et al.*, "IMU-based classification of Parkinson's disease from gait: A sensitivity analysis on sensor location and feature selection," *IEEE J. Biomed. Health Informat.*, vol. 22, no. 6, pp. 1765–1774, Nov. 2018.

[13] Y. Ma *et al.*, "Investigation of gait characteristics in glaucoma patients with a shoe-integrated sensing system," in *Proc. IEEE Int. Conf. Pervasive Comput. Commun. Workshops (PerCom Workshops)*, St. Louis, MO, USA, USA, Mar. 2015, pp. 433–438.

[14] Y. Ma, R. Fallahzadeh, and H. Ghasemzadeh, "Toward robust and platform-agnostic gait analysis," in *Proc. 12th IEEE Int. Conf. Wearable Implantable Body Sensor Netw. (BSN)*, Cambridge, MA, USA, Jun. 2015, pp. 1–6.

[15] Y. Ma, N. Amini, and H. Ghasemzadeh, "Wearable sensors for gait pattern examination in glaucoma patients," *Elsevier Microprocess. Microsyst.*, vol. 46, no. 5, pp. 67–74, 2016.

[16] T. Nakamura, "Quantitative analysis of gait in the visually impaired," *J. Disability Rehabil.*, vol. 19, no. 5, pp. 194–197, 1997.

[17] C. Prakash, R. Kumar, and N. Mittal, "Automated detection of human gait events from conventional videography," in *Proc. Emerg. Trends Commun. Technol. (ETCT)*, Dehradun, India, Nov. 2016, pp. 1–6.

[18] A. R. Anwary, H. Yu, and M. Vassallo, "An automatic gait feature extraction method for identifying gait asymmetry using wearable sensors," *Sensors*, vol. 18, no. 2, p. 676, Feb. 2018.

[19] M. Muaaz and R. Mayrhofer, "An analysis of different approaches to gait recognition using cell phone based accelerometers," in *Proc. Int. Conf. Adv. Mobile Comput. Multimedia*, Vienna, Austria, 2013, p. 293.

[20] D. Gafurov, K. Helkala, and T. Søndrol, "Gait recognition using acceleration from MEMS," in *Proc. 2st Int. Conf. Availability, Rel. Secur.*, Apr. 2006, p. 6.

[21] C. Nickel, M. O. Derawiy, P. Boursy, and C. Busch, "Scenario test of accelerometer-based biometric gait recognition," in *Proc. 3rd Int. Workshop Secur. Commun. Netw. (IWSCN)*, Gjøvik, Norway, May 2011, pp. 15–21.

[22] S. Jiang, X. Wang, M. Kyrarini, and A. Gräser, "A robust algorithm for gait cycle segmentation," in *Proc. 25th Eur. Signal Process. Conf. (EUSIPCO)*, Kos, Greece, Aug. 2017, pp. 31–35.

[23] K. Kong and M. Tomizuka, "Smooth and continuous human gait phase detection based on foot pressure patterns," in *Proc. IEEE Int. Conf. Robot. Autom.*, Pasadena, CA, USA, May 2008, pp. 3678–3683.

[24] Y. Qi, C. B. Soh, E. Gunawan, K.-S. Low, and R. Thomas, "Assessment of foot trajectory for human gait phase detection using wireless ultrasonic sensor network," *IEEE Trans. Neural Syst. Rehabil. Eng.*, vol. 24, no. 1, pp. 88–97, Jan. 2016.

[25] K. Sugandhi, F. F. Wahid, and G. Raju, "Detection of human gait cycle: An overlap based approach," in *Proc. Infocom Technol. Unmanned Syst. (Trends Future Directions) (ICTUS)*, Dubai, UAE, Feb. 2018, pp. 1–3.

[26] A. Świtoński, A. Michalczuk, H. Josiński, A. Polański, and K. Wojciechowski, "Dynamic time warping in gait classification of motion capture data," *Int. J. Comput. Inf. Eng.*, vol. 6, no. 11, pp. 306–314, 2012.

[27] T. A. Wren, K. P. Do, S. A. Rethlefsen, and B. Healy, "Cross-correlation as a method for comparing dynamic electromyography signals during gait," *J. Biomech.*, vol. 39, no. 14, pp. 2714–2718, Dec. 2005.

[28] N. V. Boulgouris, K. N. Plataniotis, and D. Hatzinakos, "Gait recognition using dynamic time warping," in *Proc. IEEE 6th Workshop Multimedia Signal Process.*, Siena, Italy, Sep. 2008, pp. 263–266.

[29] H. R. Gonçalves, R. Moreira, A. Rodrigues, G. Minas, L. P. Reis, and C. P. Santos, "Real-time tool for human gait detection from lower trunk acceleration," in *Proc. Trends Adv. Inf. Syst. Technol. (WorldCIST)*, Cham, Switzerland: Springer, 2018.

[30] M. Benoussaad, B. Sijobert, K. Mombaur, and C. A. Coste, "Robust foot clearance estimation based on the integration of foot-mounted imu acceleration data," *Sensors*, vol. 16, no. 1, p. 12, 2016.

[31] M. Patterson and B. Caulfield, "Using a foot mounted accelerometer to detect changes in gait patterns," in *Proc. 35th Annu. Int. Conf. IEEE Eng. Med. Biol. Soc. (EMBC)*, Osaka, Japan, Jul. 2013, pp. 7471–7475.

[32] J. Rueterbories, E. G. Spaich, B. Larsen, and O. K. Andersen, "Methods for gait event detection and analysis in ambulatory systems," *Med. Eng. Phys.*, vol. 32, no. 6, pp. 545–552, Jul. 2010.

[33] M. Patterson and B. Caulfield, "A novel approach for assessing gait using foot mounted accelerometers," in *Proc. PervasiveHealth*, May 2011, pp. 218–221.

[34] M. Sarmini. *Understanding Normal and Pathological Gait*. Accesssed: Oct. 2015. [Online]. Available: http://www.medschool.lsuhsc.edu/physical_medicine/PPT/Normal_Pathological_Gait.ppt

[35] M. Murray, A. Drought, and R. Kory, "Walking patterns of normal men," *J. Bone Joint Surg.*, vol. 46, no. 2, pp. 335–360, 1964.

[36] M. P. Murray, R. C. Kory, and S. B. Sepic, "Walking patterns of normal women," *Arch. Phys. Med. Rehabilation*, vol. 51, no. 11, pp. 637–650, 1970.

[37] N. Otsu, "A threshold selection method from gray-level histograms," *IEEE Trans. Syst., Man, Cybern. Syst.*, vol. 9, no. 1, pp. 62–66, Feb. 1979.

[38] G. Labiris, A. Giarmoukakis, and V. P. Kozobolis, "Quality of life (QoL) in glaucoma patients," *Glaucoma Basic Clin. Concepts*, vol. 1, no. 14, pp. 307–308, Nov. 2011, doi: 10.5772/25122.

[39] H. A. Quigley and A. T. Broman, "The number of people with glaucoma worldwide in 2010 and 2020," *Brit. J. Ophthalmol.*, vol. 90, no. 3, pp. 262–267, 2006.

[40] *The Glaucoma Foundation*. Accesssed: Oct. 10, 2015. [Online]. Available: http://www.glaucomafoundation.org

[41] P. Ramulu, "Glaucoma and disability: Which tasks are affected, and at what stage of disease?" *Current Opinion Ophthalmol.*, vol. 20, no. 2, pp. 92–98, Jun. 2018.

[42] J. Green, A. Forster, and J. Young, "Reliability of gait speed measured by a timed walking test in patients one year after stroke," *Clin. Rehabil.*, vol. 16, no. 3, pp. 306–314, Jun. 2002.

[43] A. Burns *et al.*, "SHIMMER—A wireless sensor platform for noninvasive biomedical research," *IEEE Sensors J.*, vol. 10, no. 9, pp. 1527–1534, Sep. 2010.

[44] A. Willig, "Recent and emerging topics in wireless industrial communications: A selection," *IEEE Trans. Ind. Informat.*, vol. 4, no. 2, pp. 120–124, May 2008.

[45] M. A. Buccino and J. A. Weddell, "Rett syndrome—A rare and often misdiagnosed syndrome: Case report," *Pediatric Dentistry*, vol. 11, no. 2, pp. 151–157, 1989.

[46] A. Scruggs, "Rett syndrome: Characteristics, causes, and treatment," vol. 12, no. 4, pp. 1–15, Jul. 2009. Accessed: Jul. 2009. [Online]. Available: https://www.lynchburg.edu/wp-content/uploads/volume-4-2009/ScruggsA-Rett-Syndrome-Characteristics-Causes-Treatment.pdf

[47] J. L. Neul *et al.*, "Rett syndrome: Revised diagnostic criteria and nomenclature," *Ann. Neurol.*, vol. 68, no. 6, pp. 944–950, Dec. 2010.

[48] M. Chahrour and H. Y. Zoghbi, "The story of rett syndrome: From clinic to neurobiology," *Neuron*, vol. 56, no. 3, pp. 422–437, Nov. 2007.
[49] M. Magno, D. Boyle, D. Brunelli, E. Popovici, and L. Beninii, "Ensuring survivability of resource-intensive sensor networks through ultra-low power overlays," *IEEE Trans. Ind. Informat.*, vol. 61, no. 2, pp. 946–956, May 2014.

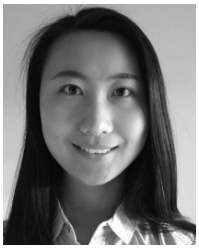

Yuchao Ma received the B.S. degree in software engineering from Xidian University, China, and the M.Sc. degree in computer science from State University of New York at Albany, NY, USA. She is currently pursuing the Ph.D. degree in computer science with Washington State University. Her research focus is on non-parametric and transfer learning algorithm development for autonomous wearable computing.

Zhila Esna Ashari received the B.Sc. degree in electrical engineering from the University of Tehran, Tehran, Iran, and the M.Sc. degree in electrical engineering and communications from the Sharif University of Technology, Tehran, Iran. She is currently pursuing the Ph.D. degree in computer science with Washington State University, Pullman, WA, USA. Her research interests are machine learning and data mining and their applications in bioinformatics and Internet of Things.

Mahdi Pedram received the B.S. degree in computer engineering from the Amirkabir University of Technology, Tehran, Iran, in 2014. He is currently pursuing the Ph.D. degree, with advanced graduate standing status, in computer engineering with Washington State University. He has been a Research Assistant with the Embedded and Pervasive Systems Laboratory since 2016. His research interests include body sensor networks, pervasive computing in healthcare, and embedded system design.

Navid Amini received the B.Sc. degree in computer engineering from Sharif University in 2007 and the M.Sc. and Ph.D. degrees in computer science from UCLA in 2010 and 2013, respectively. He is an Assistant Professor of Computer Science with California State University. He is a named inventor of three U.S. patents, two of which are licensed and moving toward commercialization. His research interests lie in mobile computing and machine learning. He was a recipient of the Edward K. Rice Outstanding Doctoral Student Award, the UCLA Chancellor's Award for Postdoctoral Research, the Alcon Young Investigator Award, the Vodafone Wireless Innovation Award, and the Innovation Fund Award.

Daniel Tarquinio is currently a Child Neurologist and an Epileptologist with the Psychiatry and Neurology Center for Rare Neurological Diseases. He is a Principal Investigator of a clinical trial on the use of triheptanoin in Rett syndrome NCT02696044 and the Lead Investigator on a study to improve outcome measures and biomarkers for Rett clinical trials. He is well known for developing Rett-specific growth charts, publications for Rett natural history study, work on the IGF-1 clinical trial, and specialization in epilepsy effects on individuals with neurodevelopmental conditions. His research interests include the treatment of epilepsy in Rett syndrome, validation and refinement of clinical research's outcomes, and identification of biometric and neurophysiological predictors of outcome.

Kouros Nouri-Mahdavi received the M.D. and M.Sc. degrees. He is currently an Associate Professor in Residence and Director of the Glaucoma Imaging Research Laboratory, Department of Ophthalmology, David Geffen School of Medicine, UCLA. His research is on functional and structural measurements for optimizing diagnosis of glaucoma, use of machine learning in them, and study of glaucoma surgical outcomes. He is a member of the AAO's Glaucoma Registry Measures Working Group and a recipient of the AAO's Achievement Award, the AGS's MAPS Grant and Early and Mid-Career Clinician Scientist Awards, the Gerald Oppenheimer Family Foundation Center for Prevention of Eye Disease Award, a CTSI Seed Grant for study of gait in glaucoma patients, the NIH K23 Award, and the UCLA Innovation Awards. He serves on the Editorial Board for the *Journal of Glaucoma*, *International Glaucoma Review*, and the *Journal of Ophthalmic and Vision Research*.

Mohammad Pourhomayoun received the B.Sc. and M.Sc. degrees from Isfahan University of Technology and the Ph.D. degree from The State University of New York at Binghamton. He was a Research Scientist with Cornell University from 2012 to 2013, a Post-Doctoral Associate with the Computer Science Department, UCLA, from 2013 to 2015, and a Technical Project Manager and the Senior Data Scientist with WANDA Inc. He is currently an Assistant Professor of Computer Science with California State University. His research interests focus on data science, machine learning, deep learning, big data analytics for healthcare applications, predictive analytics for healthcare, and wireless health technologies.

Robert D. Catena received the B.S. degree in biological sciences from the University of Alaska, Fairbanks, in 2003, and the M.S. and Ph.D. degrees in human physiology (emphasis in biomechanics) from the University of Oregon in 2005 and 2008, respectively. He was a Post-Doctoral Fellow of Occupational Biomechanics with the Harvard School of Public Health from 2008 to 2009. He was with the Physical Therapy Faculty, University of Evansville, from 2011 to 2014, where he was also the Director of the Movement Analysis Laboratory. He is currently an Assistant Professor of Kinesiology with Washington State University, Pullman, WA, USA. His research focuses on dynamic balance control and gait abnormalities that increase fall risk.

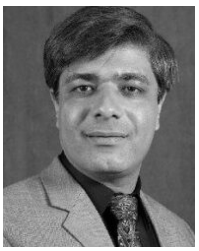

Hassan Ghasemzadeh received the B.Sc. degree from the Sharif University of Technology, Tehran, Iran, in 1998, the M.Sc. degree from the University of Tehran, Tehran, in 2001, and the Ph.D. degree from The University of Texas at Dallas, Richardson, TX, USA, in 2010, all in computer engineering. He was a Faculty Member with Azad University from 2003 to 2006, where he was the Founding Chair of the Computer Science and Engineering Department, Damavand Branch, Tehran. He was a Post-Doctoral Fellow with the West Wireless Health Institute, La Jolla, CA, USA, from 2010 to 2011, and a Research Manager with the UCLA Wireless Health Institute from 2011 to 2013. He is currently an Assistant Professor of Computer Science with the School of Electrical Engineering and Computer Science, Washington State University, Pullman, WA, USA. His research focuses on algorithm design, machine learning, and system-level optimization for embedded and pervasive systems.